9

Modeling and Identification of Parameters the Piezoelectric Transducers in Ultrasonic Systems

Pawel Fabijanski and Ryszard Lagoda
Warsaw University of Technology, Institute of Control and Industrial Electronics
Poland

1. Introduction

This chapter is dedicated to ultrasonic piezoelectric ceramic power transducers. These elements are now the most popular source of high power ultrasound and is used in many industrial applications. High power ultrasonic waves are generally used in such industrial processes as welding, acceleration of chemical reactions, scavenging in gas medium, echo sounding and underwater communication (sonar systems), picture transmission, and, above all, ultrasonic cleaning. In practice is now the most widely used the sandwich type power transducers.

Stage design power converters high power ultrasonic devices usually preceded by computer analysis of currents and voltages waveforms the elements of the system, particularly in semiconductor instruments of power. Competent representation requires the use of these waveforms of electrical models of piezoelectric ceramic transducers under the parameters of line with reality and allows to calculate the electrical operating parameters used in the layout of semiconductor switches, capacitors and reactors. Application to simulation circuit of the main generators of ultrasonic piezoelectric ceramic transducers correct model also allows analysis of different variants of control systems and regulation of voltage-frequency converters

For example the standard ultrasonic system for cleaning technology (Fig. 1) includes:

1. ultrasonic generator,
2. transducer or set of transducers,
3. cleaning tank.

Piezoelectric ceramic transducers placed in the tub generate ultrasonic waves that pass through the liquid and reach the element immersed in the tank. As a result, created in the liquid, with very high frequency, alternating areas of high and low pressure. In areas, where low pressure is forming millions of bubbles of vacuum. When the pressure in the alveoli increases and is high enough, bubbles implode, releasing enormous energy at the same time. This phenomenon is called cavitation. Emerging implosions work as a whole series of small cleaning brush. The phenomenon is spreading in all directions and causes intense but controlled detachment of particles of pollutants on the entire surface of cleaning detail. Washed away dirt particles collect on the surface of the cleaning solution from where they are blown into a nearby basin, and then be filtered and recycled.

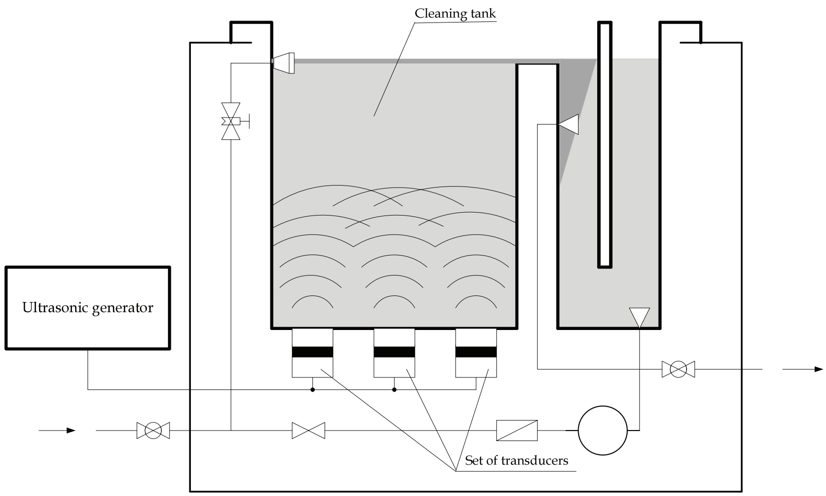

Fig. 1. Ultrasonic cleaning system

Ultrasonic cleaning is more effective in cleaning hard materials, than the cleaning of soft or porous materials. It was found that, the harder the surface, including the operation of ultrasound is more efficient. Hence, metals, glass, hard plastics well led by ultrasound and are ideally suited for ultrasonic cleaning.

2. Sandwich type transducer

In the technological equipment for cleaning, welding, etc. are generated ultrasound with high intensity and frequency from 20 kHz to 100 kHz. Currently, most teams or a single power are a source of ultrasonic piezoelectric ceramic transducers. The construction of such a transducer is shown in Fig. 2.

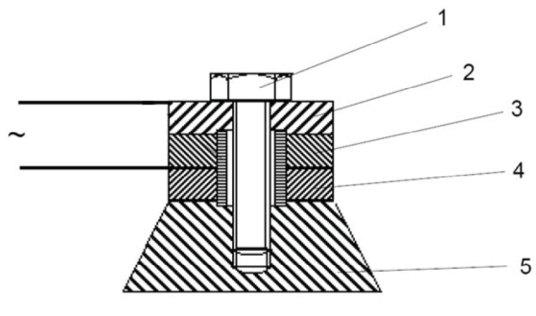

Fig. 2. Construction of sandwich type piezoelectric ceramic transducer;
1 – screw or pin settings (gripping), transmitter, 2, 5 – blocks of metal (eg. aluminum, iron, brass), 3, 4 – piezoelectric ceramic plates (cylindrical, annular)

Such transducers consists of two metal blocks (2, 5), between which are clamped to the material of the piezoelectric ceramic plate (3, 4). Metal blocks and plates are twisted with one or more screws (1). This construction has a much lower own resonant frequency compared to the same frequency of vibration plates, and what is more important allows you to generate high intensity ultrasound. Characteristic of ultrasonic power converters is that they work in a state of mechanical resonance. Thus, in this case the wave frequency of the supply voltage must be equal to the natural frequency of the transducer.

2.1 Mechanical model

Piezoelectric ceramic power converter in resonance state is a mechanically vibrating block, which can model the system with one degree of freedom shown in Fig. 3.
This model consists of mass M, which represents the mass of the whole converter, a damper with a coefficient of friction R and spring with a coefficient of mechanical sensitivity K.

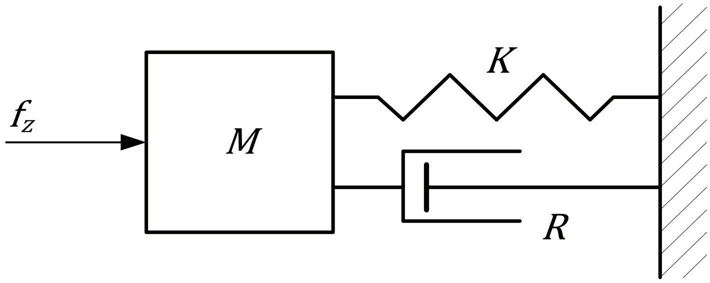

Fig. 3. The model of the mechanical oscillating system with one degree of freedom

In this system, there are four forces: the external force f_Z, the force of elasticity (Hook) f_K, the force of friction f_R and force of inertia f_M, which satisfy the equation:

$$f_Z = f_M + f_R + f_K \tag{1}$$

Assuming:
$K = \frac{1}{S}$, where S the coefficient of elasticity,
x - deviation from the equilibrium position,
v - linear velocity of particles (acoustic) dependence (1) can be written as:

$$f_Z = M\frac{d^2x}{dt^2} + R\frac{dx}{dt} + \frac{1}{K}x = M\frac{dv}{dt} + Rv + \frac{1}{K}\int_{-\infty}^{t} v d\tau \tag{2}$$

Assuming that the vibration exciting force F_Z is sinusoidal variable

$$f_Z = F_{ZM}\sin\omega t \tag{3}$$

where: F_{ZM} amplitude, and ω pulse of this force, the relationship (2) can be written as:

$$\underline{F_Z} = F_Z e^{j\omega t} = j\omega M\underline{V} + R\underline{V} + \frac{1}{j\omega K}\underline{V} \tag{4}$$

Complex mechanical impedance of the transducer is thus equal to:

$$\underline{Z_{mech}} = \frac{\underline{F_Z}}{\underline{V}} = R + j\omega M + \frac{1}{j\omega K} = R + j\left(\omega M - \frac{1}{\omega K}\right) = Z_{mech}e^{j\varphi} \tag{5}$$

The impedance module is equal to:

$$Z_{mech} = \sqrt{R^2 + \left(\omega M - \frac{1}{\omega K}\right)^2} = \sqrt{R^2 + X^2} \quad (6)$$

$$\varphi = arctg\left(\frac{X}{R}\right) \quad (7)$$

Finding a model similar to the mechanical model of electrical converter provides digital modeling of complete systems of generators supplying power electronic converters, the analysis found their current and voltage waveforms and to verify the different concepts of control algorithms of such systems.
The relationship (5) describing the complex mechanical impedance of the transducer is similar to the relationship describing the $\underline{Z_m}$ impedance of the electrical serial circuit $R_m L_m C_m$ shown on Fig. 4.

$$\underline{Z_m} = R_m + j\omega L_m + \frac{1}{j\omega C_m} = R_m + j\left(\omega L_m - \frac{1}{\omega C_m}\right) \quad (8)$$

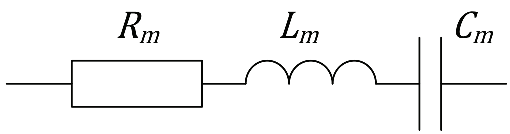

Fig. 4. Electrical serial circuit $R_m L_m C_m$

In this circuit the resistance R_m is equal to $R_m = R_s + R_a$, where R_s represents the mechanical losses of the converter, which are practically constant, and R_a the acoustic resistance, which is inversely proportional to the intensity I_a produced by the ultrasound transducer.

2.2 Electric model

Equation (5) shows that the linear velocity (molecular), vibrating transducer has the greatest amplitude when the mechanical impedance value Z_{mech} is the smallest. This condition occurs when the elastic force f_K balance the power of inertia f_M,

$$f_M + f_K = 0 \quad (9)$$

and pulse of external force f_Z, to compensate for the frictional force f_R will be equal to the pulsation resonant converter ω_m, where $\omega_m^2 = \frac{1}{M \cdot K}$.
In the piezoelectric phenomenon, the relationship between external force f_Z causing the deformation of the piezoelectric ceramic element and the intensity of the electric field E generated inside, is linear.
As for the specific thickness piezoelectric ceramic plate l we can write:

$$u = E \cdot l \quad (10)$$

then assuming a coefficient of proportionality k_p can be said that an external force k_p is proportional to the voltage that was applied to the plate.

$$f_Z = k_p u \quad (11)$$

Comparing the equation describing a serial electrical circuit $R_m L_m C_m$,

$$u = L_m \frac{d^2q}{dt^2} + R_m \frac{dq}{dt} + \frac{q}{C_m} = L_m \frac{di}{dt} + R_m i + \frac{1}{C_m} \int_{-\infty}^{t} i d\tau \quad (12)$$

of equation (2) can be seen that supplied to the circuit an electric charge is proportional to the deformation:

$$q = k_p x \quad (13)$$

Therefore meets the current relationship:

$$i = \frac{dq}{dt} = k_p \frac{dx}{dt} = k_p v \;\rightarrow\; v = \frac{1}{k_p} i \quad (14)$$

After inserting equation (11) and (14) to (2) is:

$$k_p u = \frac{M}{k_p}\frac{di}{dt} + \frac{R_m}{k_p} i + \frac{1}{k_p K} \int_{-\infty}^{t} i(\tau) d\tau \quad (15)$$

$$u = \frac{M}{k_p^2}\frac{di}{dt} + \frac{R}{k_p^2} i + \frac{1}{k_p^2 K} \int_{-\infty}^{t} i(\tau) d\tau \quad (16)$$

Since the components of the sum in equation (16) May dimension of tension is present in them can be replaced by permanent mechanical respective electrical components:

$$L_m = \frac{M}{k_p^2}, \quad R_m = \frac{R}{k_p^2}, \; C_m = k_p^2 K \quad (17)$$

2.2.1 Linear model

On the basis of equation (16) can be drawn, well-known and frequently used, an electric equivalent circuit oscillating piezoelectric ceramic transducer shown in Fig. 5.
Additional components C_e and R_e represent the electrical capacitance and resistance of the piezoelectric ceramic plate transducer.

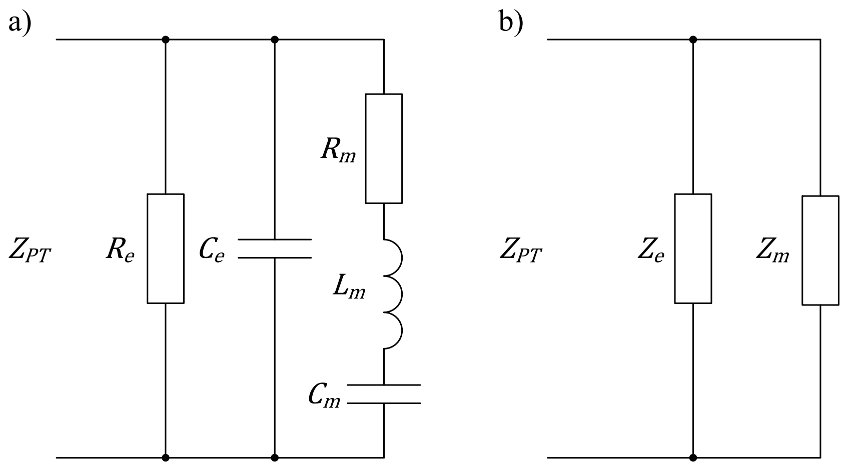

Fig. 5. Linear, a replacement wiring diagram piezoelectric ceramic transducer, Z_{PT} - Electrical impedance of the transmitter: a) a detailed diagram, b) the distribution of the branch of electrical and mechanical

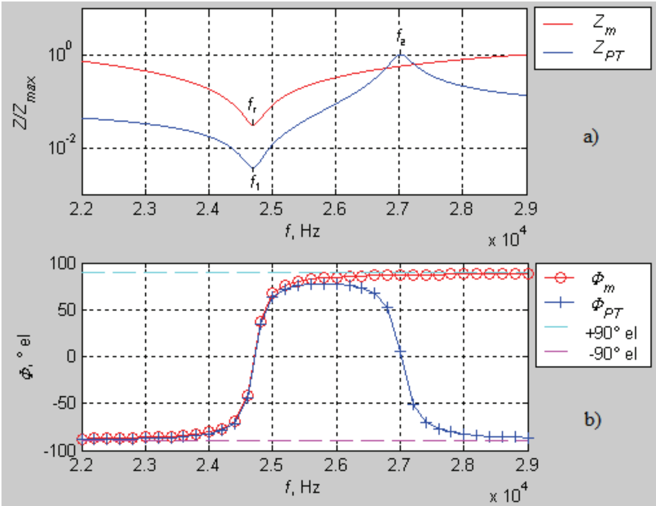

Fig. 6. Frequency characteristics of impedance modulus normalized and the phase of the mechanical industry Z_m and the entire transducerZ_{PT}

Examples of the frequency characteristics of a standard impedance modulus and phase of mechanical industry and the entire transducer is shown in Fig. 6.

When the frequency $f_1$reaches a minimum impedance Z_{PT} of the module. Near this frequency is the frequency of mechanical resonance f_r.

Resistance $R_m$can be divided into two parts:

$$R_m = R_s + R_a \tag{18}$$

where R_s represents the mechanical losses of the converter, which are practically constant, and R_a the acoustic resistance.

Presented in this chapter, a linear model of the piezoelectric ceramic transducer is not mapped correctly the actual frequency characteristics of the transmitter. Frequency response of linear model is much wider than in the actual transmitter. This is important in the process of creating digital models and design of ultrasonic generators.

2.2.2 Non-linear model

As mentioned above, the linear model presented in Fig. 5 does not correctly reproduces the frequency characteristics of the transmitter. This feature can be eliminated by supplementing the model with two non-linear electrical resistance R_{m1f} and R_{m2f} the accompanying in mechanical industries, as shown in Fig. 7.

The resultant mechanical resistance R_{mwf} in the industry is thus equal to:

$$R_{mwf} = \frac{(R_m + R_{m1f})R_{m2f}}{R_m + R_{m1f} + R_{m2f}} \tag{19}$$

Assuming that

$$R_{m1f} = R_{m1}\left(\frac{|f_r - f|}{f_r}\right)^n \tag{20}$$

$$R_{m2f} = \frac{R_{m2}}{\left(1+\frac{|fr-f|}{fr}\right)^m} \tag{21}$$

the current state of the branch of mechanical resonance, which is proportional to the speed of molecular v still is determined by the resistance R_m because, $R_{m1f}(f_r) = 0$ and $R_{m2f}(f_r) \to \infty$.

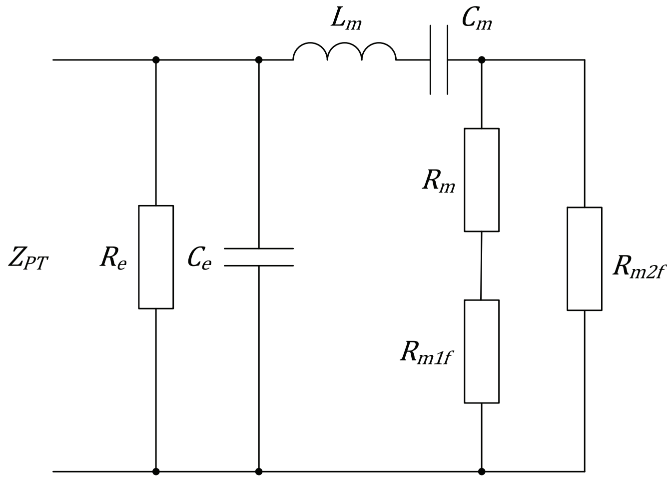

Fig. 7. Non-linear electrical model of piezoelectric ceramic transducer

3. Admittance characteristics of sandwich type transducers

The electrical characteristics of ceramic transducer resistance R_e and electrical capacitance C_e can be determined with high accuracy on the basis of electrical measurement. Changes in these parameters while the transducer can be considered to be negligible because of the transmitter power is assumed that the C_e and R_e are fixed. Parameters of dynamic branch $R_m C_m L_m$ of power piezoelectric ceramic transducer model electric are not physically measurable. We can only designate empirically. Identification algorithm is therefore based on numerical calculations. Input parameter for these calculations is the image of the actual characteristics of the transducer admittance.

Example characteristics of the actual and approximated admittance converter a resonance frequency around 25 kHz are shown in Fig. 8.

Assuming a digital model of the transmitter as shown in Fig. 5 the susceptance B, conductance G, admittance Y of the transducers in frequency ω function may be expressed by the following equations:

$$B(\omega) = ImY(\omega) = \omega C_e + \frac{\omega C_m(1-\omega^2 L_m C_m)}{\omega^2 C_m^2 R_m^2 + (1-\omega^2 L_m C_m)^2} \tag{22}$$

$$G(\omega) = ReY(\omega) = G_e + \frac{\omega^2 C_m^2 R_m}{\omega^2 C_m^2 R_m^2 + (1-\omega^2 L_m C_m)^2} \tag{23}$$

$$Y(\omega) = \sqrt{G(\omega)^2 + B(\omega)^2} \tag{22}$$

where $G_e = \frac{1}{R_e}$. For the resonant pulsation $\omega_m = \sqrt{\frac{1}{L_m C_m}}$ are:

$$B(\omega_m) = \frac{C_e}{\sqrt{L_m C_m}} \approx 0 \tag{25}$$

$$G(\omega_m) = \frac{1}{R_e} + \frac{1}{R_m} \approx \frac{1}{R_m} \tag{26}$$

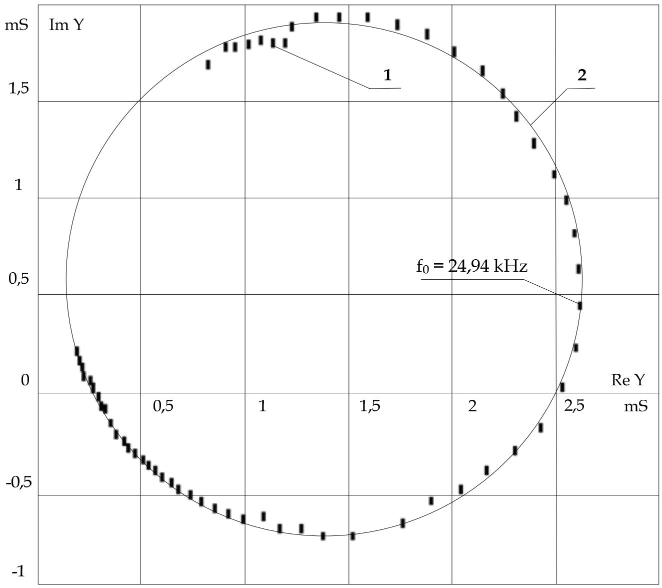

1. Real characteristic,
2. Equivalent characteristic

Fig. 8. Exemplary admittance characteristics of sandwich type transducers

4. The genetic algorithm in use to identify R_m, L_m, C_m parameters of the mechanical branch

As mentioned earlier parameters of dynamic branch $R_m L_m C_m$ of power piezoelectric ceramic transducer model electric are not physically measurable.

We can only designate empirically. Identification algorithm is therefore based on numerical calculations. Input parameter for these calculations is the image of the actual characteristics of the transducer admittance.

An example measurements of results for the transducer mechanical resonance frequency equal to about 43 kHz is locate in appendix in Table 1 and one-to-one correspondence real admittance characteristics of this transducer is shown in Fig. 9. The graph consists of points whose coordinates correspond to the conductance $G = Re(Y)$ and susceptance $B = Im(Y)$ of the converter, measured at a certain frequency.

Analysing the shape of this characteristic can be clearly observed that with increasing frequency (Figure accordance with the frequency increasing clockwise), outlines the main loop of the graph. In the general case, the image of the curve is an ellipse. This ellipse is interpolated electrical admittance characteristics of an ideal replacement transducer schedule shown in Fig. 9. It may be noted that the actual characteristics, in addition to the main loop also includes many smaller "loops" that testify to the presence of additional resonances in the transducer side. These resonances, however, will not occur in the adopted system replacement transmitter.

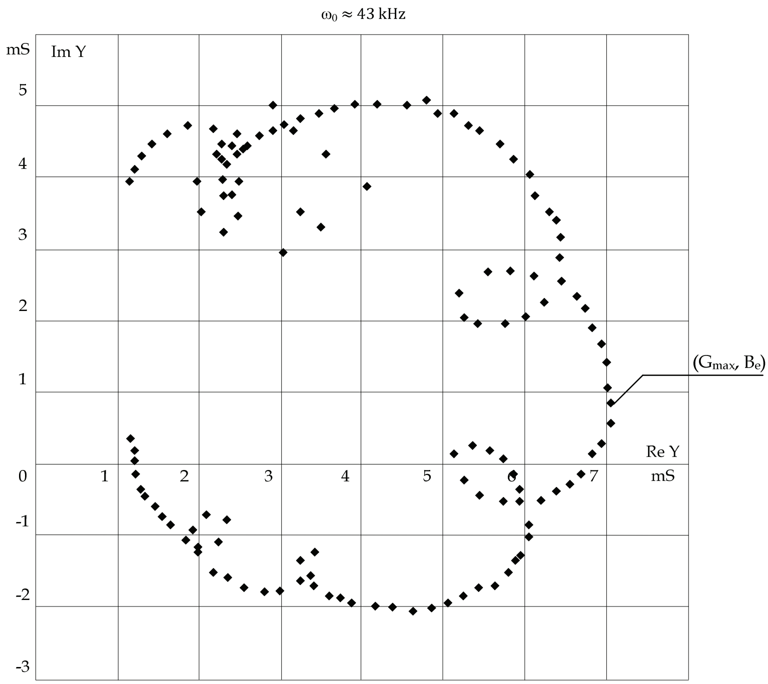

Fig. 9. Real admittance characteristics of the piezoelectric ceramic transducer

After eliminating these "loops" with the actual picture of the actual characteristics of the admittance characteristics of the transducer will be the figure presented in Fig. 10.
In Table 1 are marked in bold points, which missed the chart.

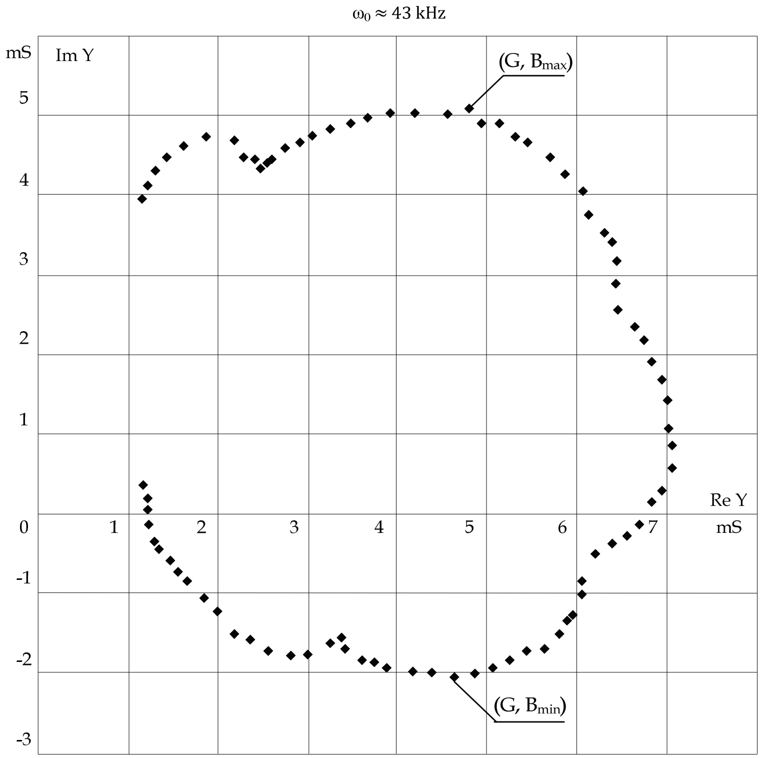

Fig. 10. The actual characteristics of the transducer after eliminating resonances fringe

The set of coordinates of the actual approximation characteristics transducer (Fig. 9) is a database for further calculations.

4.1 Calculation algorithm

Designation of alternative modes of dynamic parameters of the transmitter requires the implementation of numerical calculations and find such a set of $R_m L_m C_m$ parameters, which in a given error will allow mapping of the main loop, the actual characteristics of the transducer admittance presented Fig. 10.

One element of the identification of these parameters is a genetic algorithm. Generally one can say that the genetic algorithm is a regula - system learner who makes a certain number of iteration steps. It is a group of strict security procedures that are based on the fundamental mechanisms of biological evolution such as natural selection and inheritance. It works interactively with the environment in discrete time. The algorithm of this type of reproduction may take place subject to the diversity of the population:

- model with preload,
- measures niche

A special feature of this type is that the algorithm is not seeking a single optimal solution, but a group of cooperating the best solutions. At any time, the algorithm works evolutionary principle of survival, which is always available some of the best solutions at the moment.

As the proceedings algorithm solution to optimize and adapt to the conditions in which the algorithm works. For further calculations is always the best solutions are selected and rejected solutions are worse. Here there is a process of succession. In order to obtain optimal solutions group for further reproduction of the best solutions are selected at the time of the algorithm. It is a natural selection process occurs in nature. It is known that the probability of obtaining better result is greater if we use it to generate the best available solution than the use of inferior results. According to the law of nature and genetics "survive" the best and strongest.

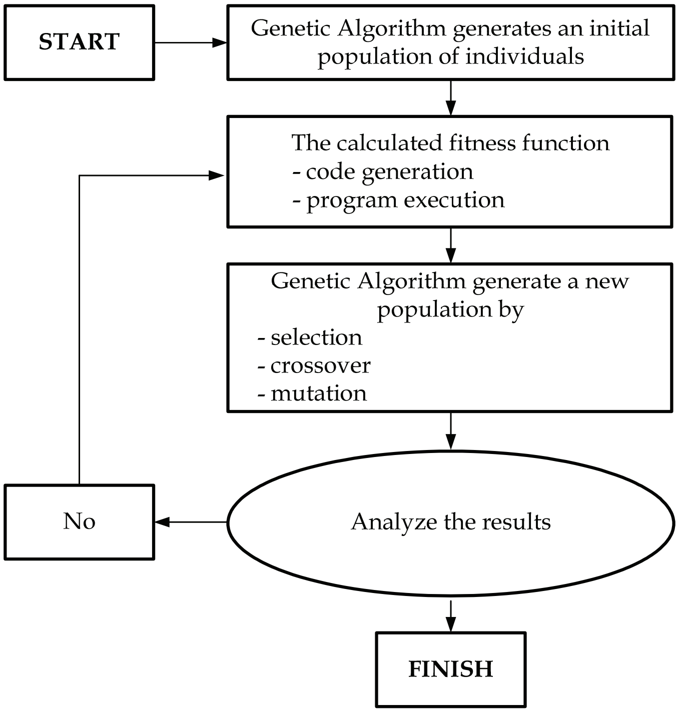

Fig. 11. Simply genetic algorithm

The genetic algorithms is a natural process of mating genes. It is no different genetic algorithm. There also are choosing the best "genes" of each solution and verify their combinations. Alongside the cross as a natural evolution is mutation, a random change in the gene. Both these processes are the values of the genetic operator.

Using the genetic algorithm, remember to keep the best balance between the transfer of genes to the next generation, and a draw solution space. Too broad conditions imposed solutions may give erroneous results in spite of every generation the best available solution at the moment. Genetic algorithm is an excellent tool to monitor and maintain the balance between these two dependencies.

The overall pattern of genetic algorithm is illustrated in Fig. 11.

Using a genetic algorithm to identify the parameters of dynamic model of the electrical branch of the transducer sandwich working near mechanical resonance is shown in Fig. 12.

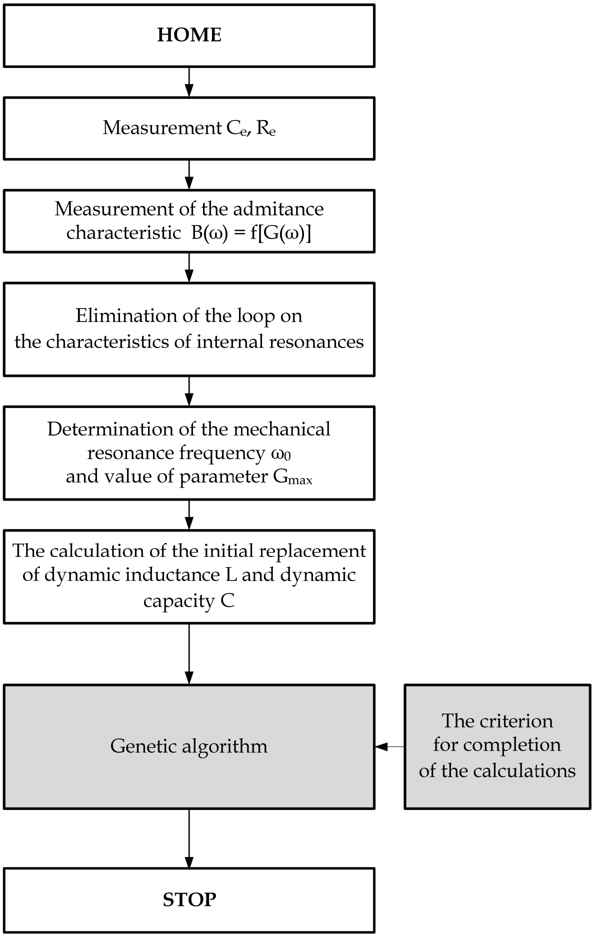

Fig. 12. Algorithm for parameter identification of dynamic model of the branch of electrical power ultrasonic transducer

The initial value of the dynamic resistance R_m is calculated by selecting the characteristics shown in Fig. 9 point with coordinates (G_{max}, B_e). In this point there is a mechanical resonance of the transducer and is a good approximation condition.

$$\omega_m^2 L_m C_m - 1 = 0 \tag{27}$$

The dependence (26) shows that the resonance:

$$G(\omega_m) = G_{max} = G_e + \frac{1}{R_m} \tag{28}$$

Therefore:

$$R_m = \frac{1}{G_{max} - G_e} \tag{29}$$

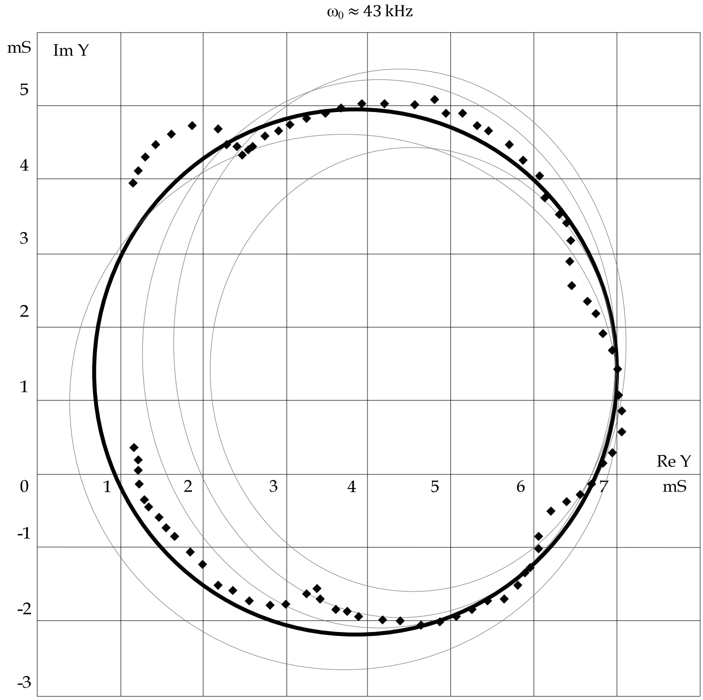

Fig. 13. Iterative improvement of the results obtained in numerical calculations and a computer simulation electric model of an sandwich type transducers

Choosing the actual characteristics of the admittance of any two points with coordinates $(G_1,\, B_1)$, $(G_2,\, B_2)$, which lie beyond the point of mechanical resonance $(\omega_1 \neq \omega_m,\ \omega_2 \neq \omega_m)$ can calculate the initial value of the replacement of mechanical capacity C_m.

Transforming the system of equations:

$$G_1 - G_e = \frac{\omega_1^2 C_m^2 R_m}{(1-\omega_1^2 L_m C_m)^2 + \omega_1^2 R_m^2 C_m^2} \tag{30}$$

$$G_2 - G_e = \frac{\omega_2^2 C_m^2 R_m}{(1-\omega_2^2 L_m C_m)^2 + \omega_2^2 R_m^2 C_m^2} \tag{31}$$

and taking into account that for G_{max} is equal to the pulsation vibrations ω_m approximate value of C_m is described by the formula:

$$C'_m = \frac{1-\frac{\omega_1^2}{\omega_m^2}}{\omega_1}\sqrt{\frac{(G_1-G_e)(G_{max}-G_e)}{1-\frac{G_1-G_e}{G_{max}-G_e}}} \tag{32}$$

$$C''_m = \frac{1-\frac{\omega_2^2}{\omega_m^2}}{\omega_2}\sqrt{\frac{(G_2-G_e)(G_{max}-G_e)}{1-\frac{G_2-G_e}{G_{max}-G_e}}} \tag{33}$$

$$C_m = \frac{C'_m + C''_m}{2} \tag{34}$$

The initial value of the replacement of mechanical inductance L_m determined from the relationship:

$$L_m = \frac{1}{\omega_m^2 C_m} \tag{34}$$

After substituting the calculated value of the $R_m L_m C_m$ and the measurement C_e, R_e the relationship (22) and (23) is determined by numerical coordinates of the points of the electrical characteristics of the admittance model for the same pulse, for which measurements of actual performance. If the error resulting from a comparison of the approximation characteristic with real characteristic (Fig. 10) is greater than the accepted values, generate a new population of C_e, R_e, $R_m L_m C_m$ parameters, repeat the calculation of coordinates of the electrical characteristics of the model and then analyze the resulting error. Calculations should be continued until the error resulting from a comparison of the characteristics shown in Fig. 10 with the characteristics of the accepted model of the electrical transducer is smaller than the set value. Measurement error should be performed in the pulsation ω changing between points B_{max} and B_{min} (Fig. 10).
Procedure described above can be used and introduces the appropriate algorithm in the DSP program simulation.

//Program piezoelectric ceramic transducer
input {Circuit parameters [R_e,C_e,R,L,C,u(t)];
Simulation parameters (t_p , t_k ,Δ,u(0))
Evolution parameters (Num,Size, NumM, Initial, NumG, stop);)
Output (t, u; t_p ; u_o =u(o);};

for (t, t_k , t++){New function form;
start initial population;}
for (integer i=1,Num,i++){New population,
Select the best}

where:
Genotype dimension: Num,
Size of the generation created by mutation: Size,
Number of the best selected genotypes for mutation: NumM,
Number of the best selected genotypes for crossing: NumC,
initial parameter mutation range: Initial

4.1.2 Description of algorithm parameters

The algorithm builds an initial population from completely random values. Each algorithm result is therefore partly random. Values implicitly included in the program when it starts in most cases produce the desired result. In order to increase the effectiveness of the algorithm we can increase the population size or quantity. This implies, however, with prolonged time needed for calculations, and thus the waiting time for results. Increasing the likelihood may lead to an erroneous finding and losing the optimal solution. In the case of reduction in population size, increased the likelihood of crossing has a better chance of getting an individual with a desired adjustment even though his speech is less certain.

Similar algorithm behaves in a situation of increasing the probability of mutation, but in this case, the result is more random.

4.1.3 Description of program code

The main application file is interface.m. He is responsible for building the interface, retrieve data from the controls and calling the functions of the buttons.

The first step is to create an initial population for genetic algorithm.

```
// INITIAL POPULATION
startpop = zeros (popsize, 2);
for i = 1: popsize
   startpop (i,:) = individual (2, max_val); / of the initial random population
end
```

The creation of the initial population is to create a matrix of population size 'number of individuals' x 'dimension of the individual', where the number of individuals is the value declared in the program window, and the dimension is equal to the number of individual factors.

The population is filled with random individuals.

The next step is to assess the population. It is used here for the sum of squared differences of the values obtained and references. Since the genetic algorithm seeks to maximize, a function of adaptation used in this case is the inverse of the sum of the squares, in addition to the square have raised to accelerate the convergence of the algorithm.

Based on the resulting evaluation, subjects were assigned to be the appropriate probability of the next population. The draw of the population makes the next feature:

```
function [new] = sel (evaluation, current) / disproportionate Roulette
global popsize;
for j = 1: popsize
   number (j, 1) = round (100 * (score (j, 3)));
end
roulette = zeros (100.2);
for i = 1:100
   Roulette (i, 1) = i;
end
// 100-point roulette wheel
all = 100;
item = popsize;
while an element> 0; / complement vector numbers in accordance with the adaptation of individual
   for a = 1: all
      Roulette (a, 2) = element;
   end
   all = all-number (element, 1);
   element = element-1;
end
// Draw elements
items = Random (popsize, 100); / draws n = popsize position
for j = 1: popsize
   number (j, 1) = roulette ((positions (j, 1)), 2); / individual in this position
end
```

```
for i = 1: popsize
   new (i,:) = current ((number (i, 1 )),:); / choose a subject to reproduce
end
```

After drawing the new population are made on the operations of crossover and mutation.

```
// CROSSING
xn = fix (popsize / 2); / number of crossover operations
remainder = mod (popsize, 2); / population parity check
steam = select (popsize); / choice pairs of interbreeding
for i = 1: xn
      [Child1 Child2] = cross ((new (pair (2 * i-1, 1 ),:)),( new (pair (2 * i, a cross ),:)));
      pox (i,:) = Child1;% first child
      pox (i + xn,:) = Child2;% second child
end
   pox (2 * xn +1,:) = new (pair (xn, 1 2 * ),:); / last rewritten without change
end
```

Crossing begins by selecting pairs of individuals, in such a way that a given individual could occur in only one hand. If the population is odd that an individual will be rewritten without change. Then it is drawn for each pair whether the operation will cross (the probability of randomly selected cross <put the probability of crossover):

- if so, part of the code is converted into fish,
- if not, individuals are no changes.

According to the function below:

```
function [Child1, Child2] = cross (A, B); / crucifixion simple
global px;
or = rand (1);
if and> px / cross check whether
   Child1 = A;
   Child2 = B;
else / crossing straight
   Child1 (1) = A (1);
   Child1 (2) = B (2);
   Child2 (1) = B (1);
   Child2 (2) = A (2);
 end
```

After the crossover operation for each individual of the population by analogy, we check if there is a mutation. If so, an individual code rate is changed to a random value according to the following function:

```
function [X] = mut (A) / mutation (replacing a randomly selected for another random value)
global max_val;
index = Random (1,2); / random mutation alleles
new = individual (1, max_val); / new value allele
A (index) = new;
X = A;
```

After mutation we get a new population, which also is subjected to evaluation of the adjustment operations, reproduction, crossover and mutation according to the number of iterations the algorithm set by the user.

Examples of results obtained in subsequent iterative steps for the transducer mechanical resonance frequency of 42.9 kHz is shown in Fig. 10.

When the next iterative step will be the condition for the completion of the calculations should be considered that the characteristics of the model shown in Fig. 5 parameters R_e, C_e and $R_m L_m C_m$ generated in the genetic algorithm in the last population of values, coincides with the actual characteristics of the interpolated transducer. The shape of this characteristic is shown in Fig. 14.

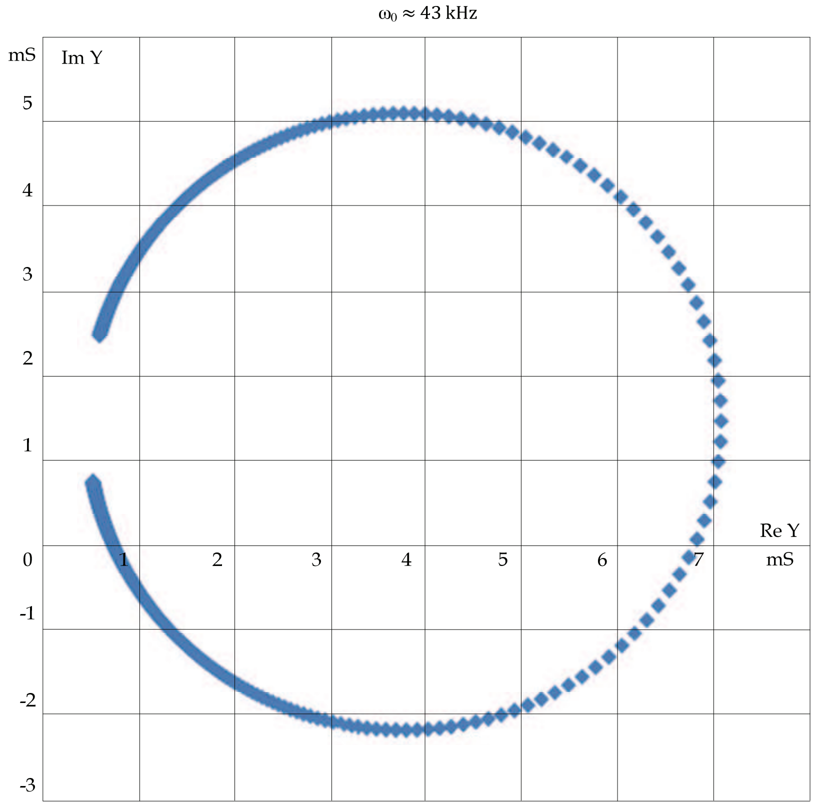

Fig. 14. Circle admittance obtained using genetic algorithm

4.2 Effect of the electrical equivalent circuit parameters on the shape characteristics of the transducer admittance

Location of figures which creates a characteristic admittance of the transducer coordinate system $B(\omega) = f[G(\omega)]$ can be determined by changing the value of capacity C_e and the loss of electrical resistance of ceramics R_e. The higher value of R_e the greater displacement figures to the right people along the conductance $G(\omega)$. If you forget in the pattern of replacement sensor resistance R_e ($R_e \rightarrow \infty$) will move to the left approximation of the characteristics. In this case, the graph will be almost tangential to the axis $B(\omega)$. Reduction in the capacity of C_e will move down the sheet, along the axis $B(\omega)$. Conductance G_{max}

value determines the width of the main loop of the graph. From relation (28) shows that the value of G_{max} decreases when the resistance R_m increases.
The impact of dynamic capacity C_m can analyze the shape characteristics of saving the relationship (22) in the form

$$B(\omega) \approx \frac{\omega C_m (1-\frac{\omega^2}{\omega_m^2})}{\omega^2 C_m^2 R_m^2 + (1-\frac{\omega^2}{\omega_m^2})} \tag{35}$$

For small, ± 2% of the pulsation untuning mechanical resonance, it can be assumed that:

$$B(\omega) \approx \frac{1-\frac{\omega^2}{\omega_m^2}}{\omega C_m R_m^2} \tag{30}$$

From relation (30) shows that reducing the value of the dynamic capacity C_m will increase susceptance system. This also applies to the maximum B_{max} and minimum B_{min}. In this case, it means that the values of B_{max} and $|B_{min}|$ increased. The difference $B_{min} - B_{min}$ is equal to the amount of main loop of the graph.
These rule changes in the electrical equivalent circuit parameters of the transducer should be used during the generation of successive populations of a set of values of R_e, C_e and $R_m L_m C_m$ genetic algorithm.

5. Conclusion

Linear model presented in Fig. 5 does not correctly reproduces the frequency characteristics of the transmitter. This feature can be eliminated by complementing the electrical model of two nonlinear resistances R_{m1f} and included R_{m2f} in the mechanical industry, as shown in Fig. 7 This is important in the process of creating digital models and design of ultrasonic generators.
The actual characteristics of the admittance is a source of transparent, condensed information about the properties and parameters of the piezoelectric ceramic transducer stimulated by the mechanical vibrations. Used to identify the dynamic parameters of $R_m L_m C_m$ and optimization of electrical parameters R_e, C_e occurring electric transducer model, genetic algorithm uses these data and represents one of many possible methods to use here. It has the advantage that it can be realized in automatic cycle.
Based on preliminary data obtained experimentally from measurements of electrical parameters (R_e, C_e) and measurements of voltage and current waveforms created image of the actual transducer admittance characteristics of $B(\omega) = f[G(\omega)]$. Genetic algorithm can find the optimal approximation of the characteristics, correction of the value of R_e, and C_e and calculation of parameters $R_m L_m C_m$ model of the electrical industry dynamic.
An important part of the described method is the proper preparation of input data. They should be given in the form of an ordered table of coordinates of points lying on the actual characteristics of the transducer according to those points that do not belong to the main loop of the graph. The process of eliminating points of the loop parasitic resonances can be implemented step by step analysis of the data included in the table of measurement results or by analyzing the image created by a set of characteristic points of $B(\omega) = f[G(\omega)]$.

Attempts to identify the parameters of a single transducer mechanical resonance frequency of 23.8 kHz and 43.2 kHz have confirmed the effectiveness of the genetic algorithm. Identification algorithm described above can be particularly useful in studies of larger groups of ultrasound transducers in high-power washing.
By introducing the necessary modifications can also be used to identify the parameters of transducers working in real conditions and to implement control systems that track the frequency of mechanical resonance.

6. Appendix

Table 1 shows selected results of detailed studies of the piezoelectric ceramic transducer mechanical resonance frequency of 42.9 kHz. Measurements were performed impedance meter HP 4192 type IMPEDANCE Analyzer. Indicated in bold letter omitted in the genetic algorithm performance admittance points beyond the main loop of the graph. The contents of Table 1 refers to Fig. 9, and Fig. 10.

f kHz	R kΩ	X kΩ	tg(φ)	φ rad	cos φ	sin φ	G mS	B mS
42,00	0,0721	-0,2338	3,2426	1,27166	0,2947	0,9556	1,204320	4,650189
42,04	0,0674	-0,2132	3,1659	1,26485	0,3012	0,9536	1,346922	4,223453
42,08	0,0703	-0,1925	2,7371	1,22052	0,3432	0,9393	1,674703	4,456680
42,12	0,0841	-0,1745	2,0750	1,12171	0,4341	0,9008	2,241050	4,963926
42,16	**0,1006**	**-0,1809**	**1,7988**	**1,06342**	**0,4859**	**0,8740**	**2,347906**	**4,296001**
42,20	**0,0921**	**-0,1763**	**1,9138**	**1,08930**	**0,4631**	**0,8863**	**2,328693**	**3,289479**
42,24	**0,0888**	**-0,1483**	**1,6705**	**1,03138**	**0,5136**	**0,8580**	**2,971594**	**3,192256**
42,28	**0,1148**	**-0,1358**	**1,1834**	**0,86919**	**0,6454**	**0,7638**	**3,630303**	**3,907909**
42,32	**0,1515**	**-0,1403**	**0,9255**	**0,74675**	**0,7339**	**0,6793**	**3,554097**	**3,487659**
42,36	**0,1501**	**-0,2015**	**1,3423**	**0,93051**	**0,5974**	**0,8019**	**2,378189**	**3,725892**
42,40	**0,1047**	**-0,2014**	**1,9231**	**1,09127**	**0,4614**	**0,8872**	**2,032128**	**3,739428**
42,44	**0,1432**	**-0,1502**	**1,0492**	**0,80942**	**0,6899**	**0,7239**	**3,323991**	**4,162891**
42,48	**0,1212**	**-0,1918**	**1,5831**	**1,00742**	**0,5340**	**0,8455**	**2,353507**	**4,431376**

f kHz	R kΩ	X kΩ	tg(φ)	φ rad	cos φ	sin φ	G mS	B mS
42,52	**0,1227**	**-0,1868**	**1,5228**	**0,98973**	**0,5489**	**0,8359**	**2,455637**	**4,700036**
42,56	**0,1041**	**-0,1800**	**1,7284**	**1,04629**	**0,5008**	**0,8656**	**2,408478**	**4,873619**
42,60	0,0992	-0,1666	1,6791	1,03365	0,5117	0,8592	2,639118	4,997220
42,64	0,0980	-0,1478	1,5079	0,98522	0,5527	0,8334	3,116930	4,959969
42,68	0,0973	-0,1351	1,3884	0,94660	0,5844	0,8114	3,510281	4,685777
42,72	0,0974	-0,1229	1,2610	0,90034	0,6213	0,7835	3,962806	4,035905
42,76	0,1005	-0,1081	1,0752	0,82162	0,6810	0,7322	4,613098	2,849480
42,80	0,1057	-0,0924	0,8738	0,71814	0,7530	0,6580	5,362597	1,944590
42,84	0,1139	-0,0752	0,6599	0,58331	0,8346	0,5508	6,115813	2,348010
42,88	0,1295	-0,0571	0,4408	0,41517	0,9150	0,4033	6,464511	2,602020
42,92	**0,1542**	**-0,0514**	**0,3331**	**0,32152**	**0,9488**	**0,3160**	**5,838341**	**1,397040**
42,96	**0,1582**	**-0,0704**	**0,4451**	**0,41880**	**0,9136**	**0,4067**	**5,274907**	**-0,305750**
43,00	0,1374	-0,0578	0,4207	0,39819	0,9218	0,3878	6,185462	-0,238180
43,04	0,1365	-0,0271	0,1982	0,19569	0,9809	0,1944	7,047725	-0,525000
43,08	0,1509	0,0070	-0,0463	-0,04622	0,9989	-0,0462	6,610636	-1,104520
43,12	0,1880	0,0084	-0,0449	-0,04483	0,9990	-0,0448	5,309238	-1,992950
43,15	0,1585	0,0133	-0,0838	-0,08362	0,9965	-0,0835	6,263456	-1,955190
43,17	0,1577	0,0283	-0,1798	-0,17789	0,9842	-0,1770	6,143423	-1,362000
43,20	0,1697	0,0661	-0,3894	-0,37135	0,9318	-0,3629	5,117705	-1,591100
43,24	0,2042	0,1018	-0,4985	-0,46245	0,8950	-0,4461	3,922151	-1,756280
43,28	**0,2579**	**0,1058**	**-0,4104**	**-0,38940**	**0,9251**	**-0,3796**	**3,319092**	**-1,271460**

f kHz	R kΩ	X kΩ	tg(φ)	φ rad	cos φ	sin φ	G mS	B mS
43,32	0,2395	0,1108	-0,4627	-0,43339	0,9075	-0,4200	3,438489	-0,718400
43,36	0,2638	0,1777	-0,6736	-0,59280	0,8294	-0,5587	2,607243	4,650189
43,40	**0,3530**	**0,2199**	**-0,6231**	**-0,55720**	**0,8487**	**-0,5288**	**2,040678**	**4,223453**

Table 1. Results of laboratory tests by the ultrasonic transducer sandwich-type of the resonance frequency around 43 kHz

7. References

Davis, L. (1991). *Handbook of Genetic Algorithms*, Van Nostrad Reinhold, New York

Gen, M. & Cheng, R. (1997). *Genetic Algorithms* & *Engineering Design,* John Wiley & Sons, New York

Rutkowski, L. (2009). Metody i techniki sztucznej inteligencji, Wydawnictwa Naukowo Techniczne PWN SA, ISBN 978-83-01-15731-9, Warsaw

Fabijański, P.& Łagoda, R. (2010). Genetic Identification of Parameters the Piezoelectric Transducers for Digital model of Power Converter in Ultrasonic Systems, In: *Piezoelectric Ceramics*, Ernesto Suaste-Gomez (Ed.) pp. 129-144, Scyio, ISBN 978-953-307-122-0, Rijeka, Croatia

Fabijański, P. & Łagoda, R. (2004). Theoretical and Experimental Analysis of Series Resonant Converter in Technical Cleaning System, Elektronika 5th International Conference MECHATRONICS 2004, No. 8-9, (September 2004) pp. 164-167, ISSN 0033-2089

Fabijański, P. & Łagoda, R. (2007). Digital Model of Series Resonant Converter with Piezoelectric Ceramic Transducers and Fuzzy Logic Control, In: *Adaptive and Natural Computing Algorithms - 8th International Conference, ICANNGA 2007, Warsaw, Poland 2007, Proceedings, Part I*, Beliczynski, B.; Dzielinski, A.; Iwanowski, M. & Ribeiro B., pp. 642-648, Springer, ISBN-13 978-3-540-71589-4, ISBN-10 540-71589-4, Springer Berlin Heidelberg New York

Fabijański, P. & Łagoda, R. (2007). Genetic identification of parameters the piezoelectric ceramic transducers for cleaning system, In: *Recent Advances in Mechatronics*, Jablonski, R.; Turkowski, M. & Szewczyk, R., pp. 16-21, Springer, ISBN-13 978-3-540-73955-5, Springer Berlin Heidelberg New York

Fabijański, P. & Łagoda, R. (2007). Series Resonant Converter with Piezoelectric Ceramic Transducers and Fuzzy Logic Control with Genetic Optimization, *Proceeding of Region 8 IEEE The International Conference on Computer as a Tool EUROCON 2007,* pp. 1884-1888, ISBN 1-4244-0813-X, Poland, September 2007, IEEE Catalog number: 07EX1617C, Warsaw

Fabijański, P. & Łagoda, R. (2008). Genetic Identification of Parameters the Sandwich Piezoelectric Ceramic Transducers for Ultrasonic Systems, *Proceeding of 13th International Power Electronics and Motion Control Conference EPE-PEMC2008*, CD-

ROM, ISBN: 978-1-4244-1742-1 (CD-ROM) , Poland, September 2008, IEEE Catalog Number CFPO834A-CDR, Poznań

Łagoda, R. & Fabijański, P. (2008). On Line PID Controller Using Genetic Algorithm and DSP PC Board, Proceding of 13th International Power Electronics and Motion Control Conference EPE-PEMC2008, CD-ROM, ISBN: 978-1-4244-1742-1 (CD-ROM) , Poland, September 2008, IEEE Catalog Number CFPO834A-CDR, Poznań

Wnuk, P. (2004). Genetic optimization of structure and parameters of TSK fuzzy models, *Elektronika 5th International Conference MECHATRONICS 2004*, No. 8-9, (September 2004), pp. 1-3, ISSN 0033-2089

Goldberg, D. (1999). Genetic Algorithms in Search, Optimization amd Machine Learning.Addison-Wesley, reading, MA

Man, K.F. & Tang, K.S. & Kwong, S. (1999). Genetic Algorithms: Concepts and Designs. Springer-Verlag London-UK

Hajela, P. & Lin, C.Y. (1992). Genetic search strategies in multicriterion optimal design.Structural Optimization,4: 99-107

Randy, L. & Sue, E. (2004). Practical Genetic algorithms. Published by John Wiley & Sons,Inc., Hoboken, Wiley-Interscience

Fathi, H. (2004). Design and simulation of a new controller for resonant operation of piezoelectric ultrasonic tools. Teheran: 19th International Power System Conference, 2004, p.1-6.

Fernandez, J. M. (2008). Adaptive control of ultrasonic motors using the maximum power point tracking method. Beijing: UFFC IEEE Conference, 2008, p.1823-1826.

Fröhleke, N. (2004). Inverter topologies for ultrasonic piezoelectric transducers with high mechanical q-factor. IEEE 35th Annual Power Electronics Specialists Conference, 2004, p.2736-2741.

Prokic, M.(2004). Piezoelectric transducers modeling and characterization. Le Locle: MP Interconsulting, 2004.

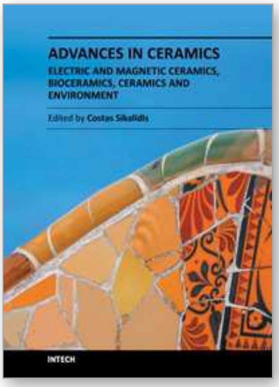

Advances in Ceramics - Electric and Magnetic Ceramics, Bioceramics, Ceramics and Environment

Edited by Prof. Costas Sikalidis

ISBN 978-953-307-350-7
Hard cover, 550 pages
Publisher InTech
Published online 06, September, 2011
Published in print edition September, 2011

The current book consists of twenty-four chapters divided into three sections. Section I includes fourteen chapters in electric and magnetic ceramics which deal with modern specific research on dielectrics and their applications, on nanodielectrics, on piezoceramics, on glass ceramics with para-, anti- or ferro-electric active phases, of varistors ceramics and magnetic ceramics. Section II includes seven chapters in bioceramics which include review information and research results/data on biocompatibility, on medical applications of alumina, zirconia, silicon nitride, ZrO2, bioglass, apatite-wollastonite glass ceramic and b-tri-calcium phosphate. Section III includes three chapters in applications of ceramics in environmental improvement and protection, in water cleaning, in metal bearing wastes stabilization and in utilization of wastes from ceramic industry in concrete and concrete products.